UDC627.338

Design of Multi-Buoy Mooring Berth

Kinji Sekita*1 Kazuto Nishimura*1
Tadashi Torii*1

Abstract:

The Kuji Underground Oil Storage Terminal adopts a unique six-point mooring berth for tanker mooring in place of the conventional fixed berth. The reason is an extremely small number of days worked per year for oil loading and unloading. When a tanker moored at multiple points is exposed to waves, winds, and tidal currents, it sways and yaws under constant external forces. It moves with respect to the point of equilibrium over a long period corresponding to the intrinsic period of floating bodies and over a short period corresponding to the wave period. A design technique was developed for estimating the maximum tanker motions by the time history response analysis of long-period motions with three degrees of slow drift oscilation and six degree of short-period oscilation and for computing the maximum mooring force of the mooring lines, while considering the nonlinear load-elongation relationship of the mooring lines and the contact of the anchor cables and sinkers with the sea bed. The design of the mooring buoy berth, including the comparison of the computational results with the experimental results, is described.

1. Introduction

A mooring facility will be constructed offshore at a water depth of 23.3 m and above a submarine manifold at the end of a 2.2 km long pipeline from an on-land riser in front of an underground oil storage terminal in Kuji City, Iwate Prefecture, north of Tokyo (see **Fig. 1**). The multiple-point mooring buoy berth consists of six buoy moorings, one stern swamp mooring, two floating rubber hoses for 50,000 to 100,000 DWt tankers, and of a structure to fix these devices.

Fig. 2 shows a single-point mooring buoy unit, a component of the six-point buoy mooring system. It consists of a 6.6 m diameter and 3.05 m high buoy, an anchor cable, a 20 ton intermediate sinker, two ground anchor cables, and two 45,000 lbs anchors. The buoy is provided with a quick-release hook, a boat

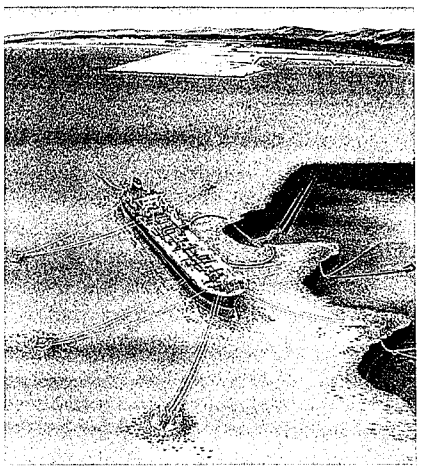

Fig. 1 Offshore multiple-point mooring buoy berth

*1 Civil Engineering & Marine Construction Division

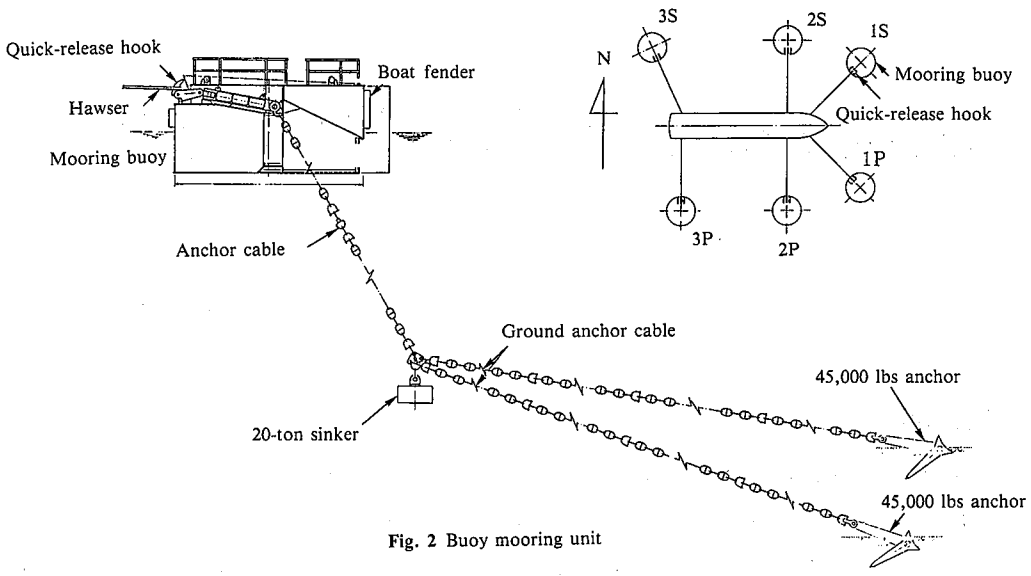

Fig. 2 Buoy mooring unit

fenders, and other necessary devices. Three such mooring buoys are arranged on each side of the tanker in the outgoing condition as shown in **Fig. 1**.

Oceanographic phenomena attack the tanker generally in the southeast direction on the seaward side. A swamp mooring unit, composed of wire rope of such a type as not to interfere with the entry of the tanker into the berth, is added against wind from the land in the winter season.

2. Design of Multiple-Point Mooring Buoy Berth

The multiple-point mooring buoy berth was designed according to the procedure shown in **Fig. 3**. Three tanker sizes, 50,000, 75,000, and 100,000 DWt, were studied for the ballasted and full loaded conditions. In the study, a water depth of -23.3 m and tidal range of $+1.8$ m were adopted.

The design oceanographic phenomena are as listed in **Table 1**. The mooring operation is assumed to be conducted within the limits of the oceanographic phenomena conditions concerned. Waves in the northeast through southeast directions and winds and tidal currents in all directions were studied in combination. A mooring buoy unit, which comes a single-point mooring state when no tanker is moored, was also designed to guard against the oceanographic phenomena whose recurrence probability is calculated to be once every 100 years.

3. Analysis of Multiple-Point Mooring Buoy Berth with Moored Tanker

3.1 Description of numerical analysis method

The method of numerical analysis for the case in which a tanker is moored to the berth is shown in **Fig. 4**. Motion equations for the wave exciting force which is a short-period load, for the wind pressure due to the fluctuating wind which is a long-period load, and for the slowly varying drift force in irregular waves which is another long-period load, were sequentially solved. The results of the sequential analyses of short-period loads were added to those of the sequential analyses of long-period loads. The time history data of overall tanker motions and mooring line tension responses were obtained accordingly.

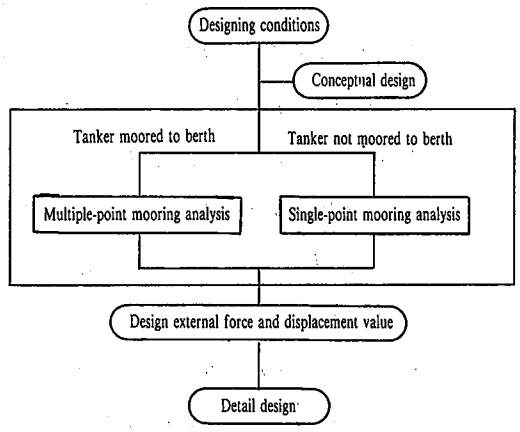

Fig. 3 Designing procedure for multiple-point mooring buoy berth

Table 1 Oceanographic phenomena for multiple-point mooring buoy berth

	Tanker moored to berth	Tanker not moored to berth
Significant wave height (maximum wave height)	1.5 m	8.5 m (13.5 m)
Wind velocity	15 m/s	38 m/s
Tidal current velocity	0.1 m/s	0.1 m/s
Tsunami	—	3.25 m/s

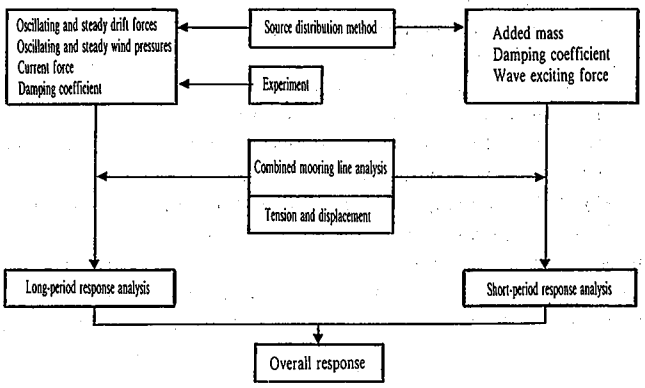

Fig. 4 Method of numerical analysis with tanker moored to berth

This method of numerical analyses is described below.

(1) The short-period motions were considered by six degrees of freedom. The hydrodynamic force coefficients and wave exciting force in the motion equations were determined by the three dimensional source distribution method.

(2) The long-period motions were studied taking into consideration three degrees of freedom, i.e., sway, surge and yaw. The added mass coefficient and wave drift force in the motion equations were determined by the three-dimensional source distribution method. The damping coefficients were based on values obtained by free oscillation experiments in calm water[1]. The wind loads were computed from the experimentally determined wind drag force coefficients.

(3) The hawser load-elongation nonlinearity, buoy buoyancy change, and sinker rise from and fall to the sea bottom were taken into account when determining the restoring characteristics of the mooring lines.

(4) The numerical analyses were performed by the Newmark β method at time intervals of 0.5 s for 1 to 2 h.

3.2 External forces acting on tanker

Each external force component was computed according in principle to the "Technical Standards for Port and Harbor Facilities and Commentary".

3.2.1 Load due to tidal current

The tidal current force (F) acting on the tanker is calculated by

$$F=\frac{1}{2}\rho_w V_c^2 AC \qquad \cdots\cdots(1)$$

where ρ_w is density of sea water; V_c is tidal current velocity; A is projected area of tanker below the surface of water; and C is value dependent on relative tidal current direction, the depth of water and draft.

3.2.2 Wind load

The wind load acting on the tanker is resolved into surge, sway and yaw components (Fx, Fy, Mz, respectively) and computed by

$$\begin{Bmatrix} Fx \\ Fy \\ Mz \end{Bmatrix} = \frac{1}{2}\rho_a \begin{Bmatrix} C_{DX}At \\ C_{DY}As \\ C_{Dn}AsL \end{Bmatrix} |U+u(t)|\cdot(U+u(t)) \qquad \cdots\cdots(2)$$

where ρ_a is density of air; C_{DX}, C_{DY} and C_{Dn} are experimentally determined wind drag force coefficients of tanker; L is length of tanker; At and As are front and side projected areas of tanker above water surface, respectively; and U is 10 min average wind velocity. The fluctuating wind velocity u(t) was given by a Furier series by using the amplitude calculated from a wind spectral density of the Davenport type and the phase determined from random number generation.

3.2.3 Wave drift force

The constant components and fluctuation components of the wave drift force ($\tilde{F}x$, $\tilde{F}y$, $\tilde{M}z$) are simultaneously given by[2]

$$\begin{Bmatrix} \tilde{F}x(t) \\ \tilde{F}y(t) \\ \tilde{M}z(t) \end{Bmatrix} = \begin{Bmatrix} \overline{Fx} \\ \overline{Fy} \\ \overline{Mz} \end{Bmatrix} \frac{\xi^2(t)}{\sigma^2} \qquad \cdots\cdots(3)$$

where $\{\overline{Fx}, \overline{Fy}, \overline{Mz}\}$ are constant components of wave drift force; σ^2 is variance value of irregular wave; and $\xi(t)$ is water surface elevation.

Since it is decided to separately solve the long-period and short-period responses, the solution of the long-period response equation diverges if there is a high-frequency component. Time series data simulating both wind load and wave slow drift were then Fourier-transformed, and high-frequency components greater than 0.1 Hz were cut. The resultant data were further inverse Fourier-transformed and returned to time history response data. The cut high-frequency components were similarly inverse transformed and added to the wave exciting force time history as described next.

3.2.4 Wave exciting force

The six-degrees-of-freedom wave exciting force F(t) for irregular waves is computed from the wave force magnification factor in regular waves as given by

$$F(t)=\int_0^\infty \sqrt{2S(f)\,df}\; H(f)\cos(2\pi f+\varepsilon) \qquad \cdots\cdots(4)$$

where S(f) is wave spectrum; H(f) is wave force magnification factor of regular waves; f is frequency; and ε is phase lag (random number generation). Like the fluctuating wind velocity components, the water surface elevation time history $\xi(t)$ in Eq. (3) and the wave exciting force are prepared by the Bretschneider-Mitsuyasu type wave spectra and by random number generation.

3.3 Damping coefficient

The decay of long-period motions, an important factor in this analysis, was determined taking into consideration the experimental results given in **Table 2**. Take yaw for example. Since the oscillatory waveform is small in the free oscillation experiment, the response is represented by the following oscillatory waveform of a one-degree-of-freedom system (Y(t)):

$$Y(t)=e^{-nt}\left(Y_0\cos p\sqrt{1-n^2/p}\,t + \frac{\dot{Y}_0+nY_0}{p\sqrt{1-n^2/p^2}}\sin p\sqrt{1-n^2/p^2}\,t\right) \qquad \cdots\cdots(5)$$

where p is $2\pi/T_n$; T_n is natural period; and t is time.

As shown in **Fig. 5**, the initial velocity $\dot{Y}_0$ was assumed with the initial angle Y_0 of yaw as the origin, and the natural frequency T_n and the damping index n were determined so that the experimental line should agree with the free oscillation waveform expressed by Eq. (5). Since surge appeared larger than that studied by Wichers[3], the results of Wichers were used on the conservative side. The sway of the tanker in the ballasted condition in **Table 2** was used by referring to the results of Ando et al. about

Table 2 Surge, sway, and yaw damping coefficients used for purpose of computation

	Ballasted condition	Full loaded condition
Surge C_X	10 $tm^{-1}s$	100 $tm^{-1}s$
Sway C_Y	30 $tm^{-1}s$	600 $tm^{-1}s$
Yaw C_N	5×10^4 tms	1.0×10^6 tms

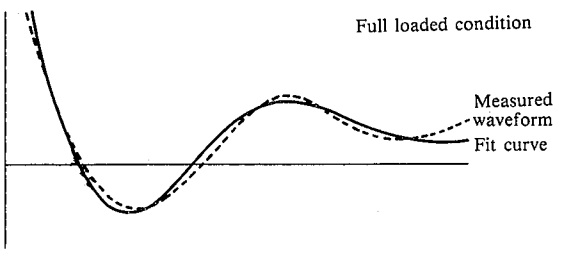

Fig. 5 Computation of damping coefficient

box-shaped flat barge. In the absence of comparable data, the smallest values of the experimental results were used for yaw.

The damping coefficient of short-period motion with respect to the significant wave height $H_{1/3}$ and the significant wave period $T_{1/3}$ was determined as follows. The curves of the damping coefficient $C_{jk}(f)$ for six components in regular waves analyzed by the three-dimensional source distribution method were precalculated. The equivalent damping coefficient $\overline{C_{jk}}$ was obtained by

$$\overline{C_{jk}}(H_{1/3}, T_{1/3}) = \frac{\int_0^\infty S(f) C_{jk}(f)\,df}{\int_0^\infty S(f)\,df} \quad \cdots\cdots(6)$$

Nonlinearity was taken into account for the roll of the tanker.

3.4 Righting force of mooring lines

When a tanker is moored to the berth, it is connected to 6.6 m diameter buoys by hawsers with a nonlinear load-elongation relation. The nonlinearity of the hawsers is given by such a curve that the hawser is elongated 10%, 15%, and 20% when tensioned to 21%, 56%, and 100% of the proof load, respectively. The weight of the sinker is 20 tons in water, and the height from the point of connection between the top surface of the sinker and the anchor cable to the bottom surface of the sinker is 6 m. **Fig. 6** shows the relationship between the horizontal tension of the hawser and the horizontal distance between the anchor and hawser in a tidal range at the lowest and highest sea levels. The slope of the curve near the mooring condition under which the hawser is tensioned to produce a horizontal force is greater at the lowest sea level. The displacement response of the tanker diminishes as a result.

3.5 Results of analysis

3.5.1 Tanker motions

Fig. 7 shows the sway and surge time history analysis results of a 100,000-DWt tanker in the ballasted condition. The oceanographic phenomena are wind acting on the tanker at a velocity of 20 m/s in a clockwise direction of 270° from the bow and irregular waves acting on the tanker with a significant height of 2.0 m by each period of 7 s in the 225° direction. As external forces, the wave drift forces are Fy is −62 tf and Mz is −850 tm, and the wind drag force coefficients C_Y and C_N are 0.66 and 0.03, respectively.

The constant external forces in this condition are that Fx is 7 tf, Fy is −118 tf, and Mz is −1,087 tm. It is evident that the tanker moves over a long period of about 130 s with the short-period components slightly superimposed so as to correspond to the 144 s natural period of sway motion.

Of the tanker motions analyzed, the maximum, average, and minimum sways may be plotted against the significant wave height as shown in **Fig. 8**. In the Figure, the bar graphs indicate the experimental values, which agree well with the analytical values except for the 1.5 m significant wave height. As the significant wave height increases, the analytical values become greater than the experimental values.

3.5.2 Tension of mooring lines

Fig. 9 shows the time history of the maximum tension of mooring lines. This diagram concerns a 100,000-DWt tanker in the ballasted condition with a wind velocity of 20 m/s (in 225° direction), significant wave height of 2 m (in 225° direction), and significant wave period of 8 s. The maximum tension decreases for the upwind or port hawsers 3P, 2P, and 1P in that order and slowly changes with practically the same phase at a period of

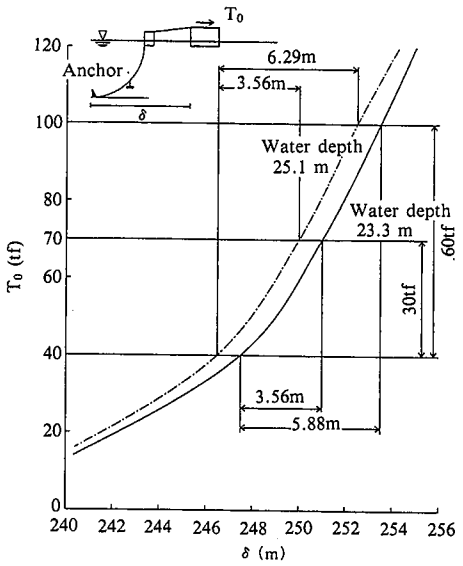

Fig. 6 Water depth and curve relating δ (horizontal distance between anchor and hawser end) to T_0 (horizontal mooring force)

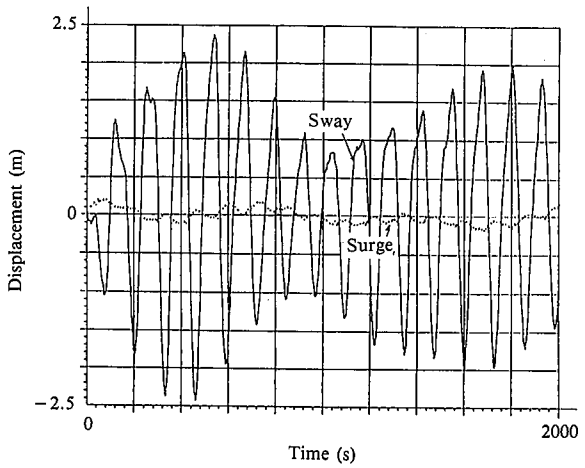

Fig. 7 Analytical results of tanker motions (sway and surge)

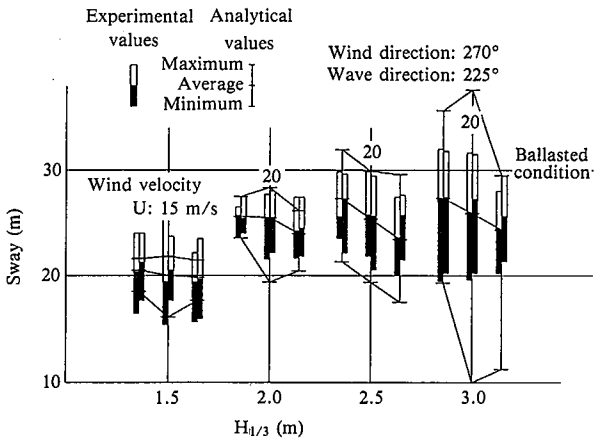

Fig. 8 Maximum sway of tanker

about 121 s, a value close to the 125 s natural period of sway.

Fig. 10 shows the maximum tension of the three mooring lines 1P through 3P in the full loaded condition with a wind velocity of 15 m/s (in 225° direction) and wave heights of 1.5 and 2 m (in 225° direction). The experimental values agree well with the analytical values.

3.5.3 Limits of mooring

Fig. 11 shows the experimental and analytical maximum tensions of mooring lines in relation to the wind velocity and significant wave height. The maximum mooring tension increases with increasing wave height and wind velocity. Since the damping coefficient of long-period tanker motion is assumed to be constant, the analytical values tend to appear slightly higher than the experimental values as the wave height increases.

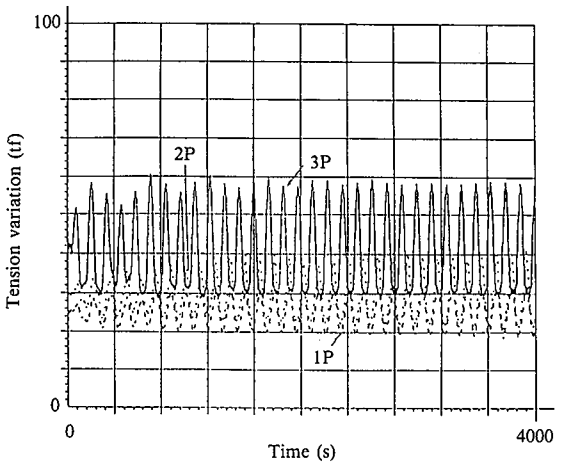

Fig. 9 Time history of tension variations

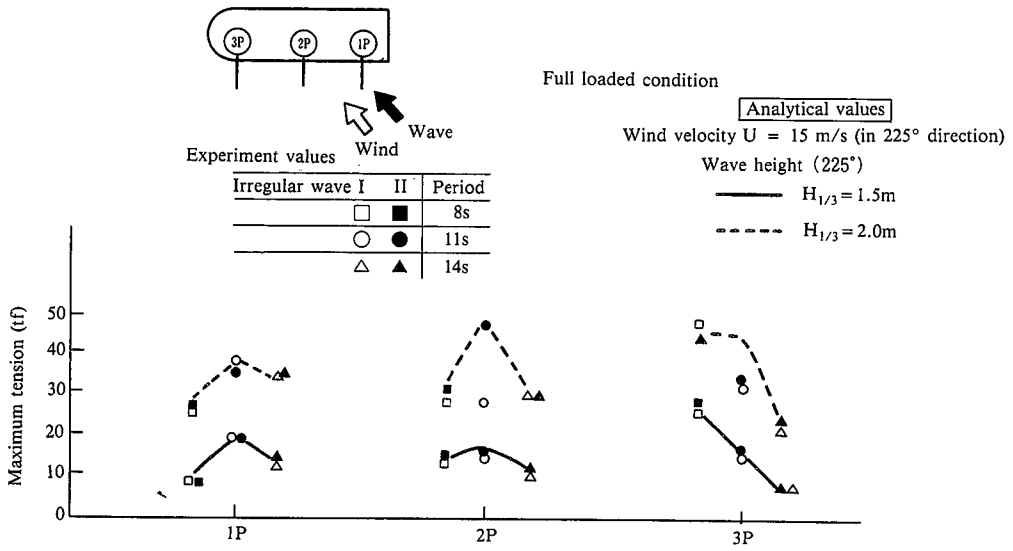

Fig. 10 Maximum tension distribution of port mooring lines

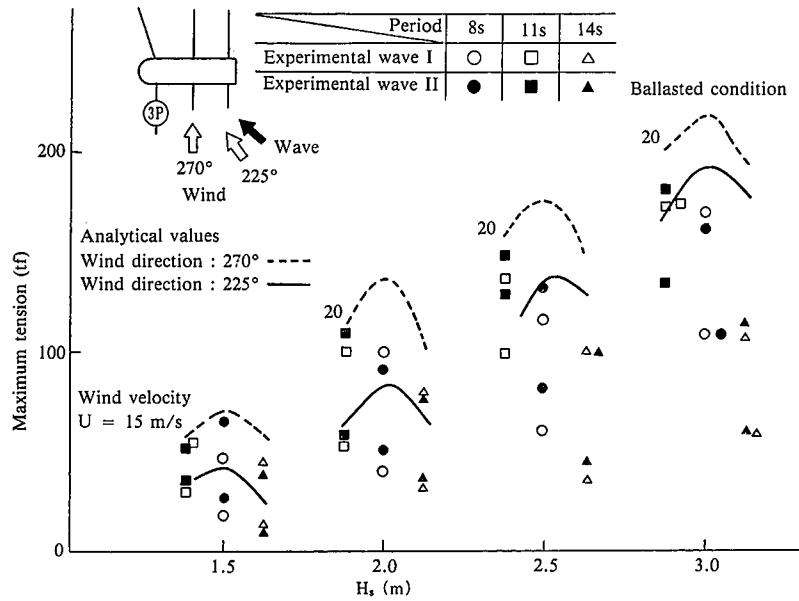

Fig. 11 Relationship between significant wave height H_s and maximum tension of mooring lines

4. Analysis of Multiple-Point Mooring Buoy Berth without Moored Tanker

Anchors at the buoy berth are installed so that each anchor can effectively exhibit its holding force in the direction of the mooring line it serves. When the tanker is not moored to the multiple-point buoy berth, the sinker located on the weather side of the anchor for the buoy in the direction of the external force as shown in **Fig. 12(a)** is liable to be dragged by the external force until it forces the anchor out of the seabed.

In case the tanker is not moored to the buoy berth, therefore, the strength of the mooring lines and the details of the anchors must be examined against the design conditions listed in **Table 1**. When the tanker is not moored to the buoy berth, the loads that act on the buoys of the berth total 1.62 tf for the tidal current force, wind load, and steady wave drift force combined. Of these force components, the wind load is predominant. Its wind drag force coefficient C_s is put at 1.0 for the buoy proper and at 1.3 for the deck structure. The drag coefficient C_d is put at 1.0 for tsunami surge, and a tidal current pressure of 5 tf is assumed to act on each buoy.

4.1 Evaluation of buoy motions

Buoy motions in regular waves were analyzed by the three-dimensional source distribution method, and the 1/1000 maximum expected value of surge with a significant wave height of 8.5 m (wave period of 14 s) was estimated at 11.25 m by the short-term statistical prediction method.

4.2 Frictional force of sinker, ground anchor cable, and anchor

As to the stability of the anchor, such an extreme case was assumed that the anchor is located behind the sinker in the direction of the external force as shown in **Fig. 12(a)**, in which position it would produce no design holding force but a mere frictional force.

In this extreme case, the frictional force is 45 tf when the coefficient of friction with the sand of the seabed is put at 0.6 for the sinker, 0.75 for the ground anchor cable, and 0.6 for the anchor. The anchor is actually buried in a hole dug in the seabed stiff soil for added safety. This frictional force of 45 tf is far greater than the tension of 5 tf when the tsunami surge arrives and the tension of 42 tf when the anchor is located behind the sinker in the direction of the external force as shown in **Fig. 12(a)**. It is also greater than the horizontal force of 41.5 tf computed taking into account the effect of tidal current in the Morison equation while assuming that the buoy does not move when tsunami as high as 15.35 m above the maximum sea level arrives. When the anchor is located before the sinker in the direction of the external force as shown in **Fig. 12(b)**, the horizontal force acting on the buoy is 57 tf. The holding force of the anchor is 142.8 tf when the holding force factor is 7. This means that the anchor will not move.

5. Items Considered for Operational Control

In the design stage, seven moorings, including a swamp mooring, were analyzed. It was found as a result that waves arriving with a significant wave height of 1.5 m (period of 9.5 s) in a direction of 225° and winds arriving at a velocity of 15 m/s in a direction of 270° constitute critical conditions. The maximum design tension and other factors may be summarized as shown in **Table 3**. The tension of mooring members is calculated from the horizontal tension values in **Table 3**.

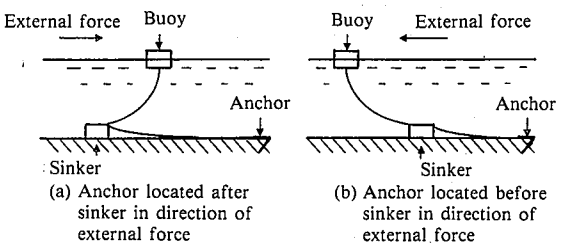

Fig. 12 Relationship among buoy, sinker, and anchor when tanker is not moored to berth

Table 3 Maximum design tension

	Tension when tanker is moored to berth (tf)	Tension when tsunami arrives (tf)	Tension when tanker is not moored to berth (tf)
3S line	11	5	57 (Anchor located before sinker)
3P line	68	5	42 (Anchor located after sinker)
Swamp type mooring line	30	—	—
Maximum tanker motion	Surge: −1.5 m Sway: +8.5 m Yaw: −0.9°		

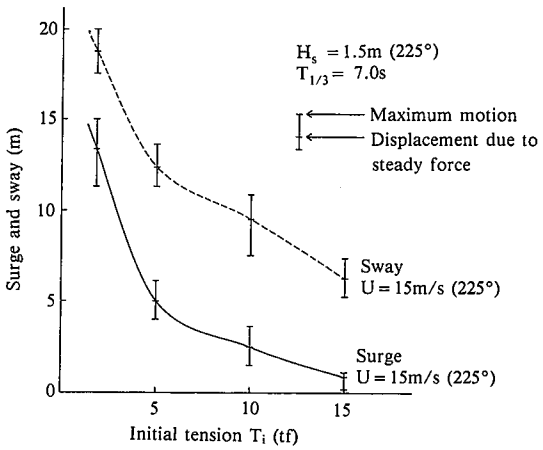

Fig. 13 Effect of initial tension of mooring lines on motion of tanker

The tanker motions, on the other hand, are analyzed for the initial tension of 15 tf. Postulating that the buoy berth may also be operated with much smaller initial tensions, response analysis was conducted by determining the long-period motion damping coefficient C as follows:

$$C = 2h\sqrt{Km} \qquad \cdots\cdots(7)$$

where h is damping constant obtained from the damping coefficient shown for the tension of 15 tf in **Table 2**; K is righting coefficient of mooring lines; and m is mass.

The results of analysis performed using the damping coefficient are as shown in **Fig. 13**. When the initial tension is 5 tf, the tanker motion increases to 13.5 m. This value falls within the permissible range of movement of the oil loading and unloading rubber hose connecting the submarine manifold and the tanker.

When the proof load of anchor cables after the service life of 20 years was estimated from corrosion weight loss and wear, it was found that the achieved safety factor was greater than the specified value of 3.

The shape, draft, surplus buoyancy, and other details of the buoys are determined so that they are not submerged when subjected to the maximum horizontal force of 68 tf and remain intact even when partly damaged.

The swamp mooring unit is composed of two wire ropes with a diameter of 33.5 mm and breaking strength of 71.1 tf, a 58 mm diameter anchor cable, a 9-ton sinker, and a 15,000-lbs ground anchor cable. It is normally placed on the seabed and is connected to the winch of the tanker when the tanker is moored to the buoy berth.

6. Conclusions

In the design of a multiple-point mooring buoy berth, the vessel motion characteristics and mooring line tensions are determined according to the slow drift of the vessel due to wave irregularity and wind fluctuation. Against long-period external forces, the multiple-point mooring buoy berth was analyzed for three degrees of freedom, i.e., surge, sway and yaw. With the addition of roll, heave and pitch against short-period loads like the wave exciting force, the time history response of the berth was computed by analyzing a total of six degrees of freedom. The computed results were superimposed on the three-degrees-of-freedom motions obtained first. The newly developed designing technique was verified through comparison with the results of experiments conducted at the Port and Harbor Research Laboratory of the Ministry of Transportation. It was confirmed as a result that the technique is high in accuracy as previously reported. It was applied to the design of the multiple-point mooring buoy berth to be constructed in the Kuji Bay. A series of numerical simulation was performed with tanker size, orientation (incoming or outgoing) and load condition, wave height, wind velocity, wind direction-wave direction combination, and other conditions as parameters. The following findings were obtained:

(1) The mooring force and vessel motion become the largest for the 100,000-DWt tanker.
(2) The orientation of the tanker does not significantly influence the maximum mooring force.
(3) The tanker motion and mooring force are greater in the ballasted condition with a greater wind load than in the loaded condition.
(4) The maximum mooring force becomes the greatest when the wind direction is 270° (in south direction) and the wave direction is 225° (in southeast direction).
(5) When the initial tension is small, the maximum tension is small, but the maximum motion is large.

References

1) Hiraishi, T., Takayama, T., Sekita, K., Torii, T.: Experimental and Numerical Study on Mooring Tension and Motion of a Tanker in a Multi-Buoy Berth. Proc. 3rd Intern. Offshore and Polar Engineering Conf. June 1993
2) Kato, S.: Simulation of Long-Period Motion and Mooring Force of Moored Floating Body in Irregular Waves. Report of Ship Research Institute. 25 (2), March 1983
3) Wichers, J.E.W.: A Simulation Model for a Single Point Moored Tanker. (797), Maritime Research Institute, Netherland